Trends in spin-transfer-driven magnetization dynamics of CoFe/AlO/Py and CoFe/MgO/Py magnetic tunnel junctions

G. Finocchio,[a] G. Consolo, M. Carpentieri, A. Romeo, and B. Azzerboni
Dipartimento di Fisica della Materia e Tecnologie Fisiche Avanzate, University of Messina, Salita Sperone 31, 98166 Messina, Italy

L. Torres and L. Lopez-Diaz
Departamento de Fisica Aplicada, Universidad de Salamanca, Plaza de la Merced s/n, 37008 Salamanca, Spain

(Received 17 October 2006; accepted 25 November 2006; published online 28 December 2006)

A spin-polarized current is able to excite magnetization dynamics in nanomagnets. A detailed theoretical study of dynamics in low and high field regimes in AlO and MgO magnetic tunnel junctions (MTJs) is presented, considering the maximum value of the applied current which comes from the breakdown voltage of the tunnel barrier. In low field regime, dynamics with a well-defined peak in frequency is observed. In high field regime, AlO MTJ presents the same behavior, while the magnetization in the MgO MTJ shows chaotic motion with a noisy spectrum. Lastly, an effect of the presence of a pinhole in the tunnel barrier is discussed. © *2006 American Institute of Physics*. [DOI: 10.1063/1.2425017]

A spin-polarized current (SPC) flowing through a nanomagnet applies torque to its magnetization that can either induce magnetization reversal or excite persistent dynamics (self-oscillations) of magnetization.[1,2] These behaviors have been experimentally observed in spin valves (SVs),[3] magnetic tunnel junctions (MTJs),[4] and point-contact geometries.[5] Concerning the MTJs, they show promise as high performance magnetic random access memory and the possibility to excite microwave oscillations, also opens important perspectives of its potential applications such as high impedance spin-transfer-driven oscillators. While the SPC necessary to invert the antiparallel state (APS) to parallel state (PS) and *vice versa* for the MTJs is comparable with that of SVs, there is a more restrictive physical limit on the maximum value of applied current due to the breakdown voltage of the barrier. In the MTJs based on MgO tunnel barrier, the high tunnel magnetoresistance (TMR) suggests that these will have a major impact on technologically relevant spintronic devices operable at room temperature and above in the near future.

In this letter, we present the results of full micromagnetic simulations which predict and show the perspectives for possible applications of magnetization dynamics driven by SPC in the two main families (MgO and AlO) of MTJs used in the "state of the art" experiments.[4]

MTJs were patterned from thin films consisting of CoFe(8 nm)/Al2O3(0.8 nm)/Py(4 nm) and CoFe(8 nm)/MgO(0.8 nm)/Py(4 nm) with an elliptical cross section (90×35 nm^2), where the CoFe and the Py are the pinned layer (PL) and the free layer (FL), respectively. We consider the easy axis of the ellipse as the x axis and the in-plane hard axis as the y axis. The simulations have been performed by solving the Landau-Lifshitz-Gilbert-Slonczewski equation,[6] including both the magnetostatic coupling between the PL and the FL and the classical Oersted field together with the standard effective field (exchange, Zeeman, anisotropy, and magnetostatic).[6] We do not consider magnetocrystalline anisotropy for the Py. The polarization function g_T, which modulates the spin-transfer torque, has been considered as proposed by Slonczewski in 2005.[7] $g_T(\theta)=0.5\,\eta_T(1+\eta_T^2\cos(\theta))^{-1}$, where η_T is the polarization factor. We also use $M_S=644\times10^3$ A/m and $M_{SP}=1.15\times10^6$ A/m for the saturation magnetizations of the FL and the PL, respectively, a damping $\alpha=0.01$, and an exchange constant $A=1.3\times10^{-11}$ J/m. We consider a positive current when it flows from the PL to the FL. We consider the orange-peel coupling negligible.[8]

From the theoretical point of view, it is well known that the MTJs (both with AlO or MgO tunnel barrier) exhibit a TMR that decreases when the applied voltage increases. On the other hand, current induced switching occurs at a large voltage, where the current must be spin polarized in order to exert a significant spin-transfer torque. A recent experimental study on MTJs with a MgO tunnel barrier shows that the polarization factor η_T is a constant function of the bias within a 10% uncertainty.[9] Starting with this experimental remark that a decrease in TMR does not indicate a decrease in the spin polarization, we consider η_T to be constant for both positive and negative currents used for our simulations. With that further hypothesis, we obtain a symmetric torque, in agreement with most of the experimental data published so far.[4,9] We use for the AlO MTJ $\eta_T=0.3$: this has been computed by fitting the experimental critical currents of the most complex structure of Ref. [10]. For the MgO MTJ, we use $\eta_T=0.7$: this value is smaller than the one obtained in the CoFe/MgO/CoFe MTJ. We consider a breakdown voltage of the tunnel barrier of 0.5 V for both the devices and a maximum resistances (APS state) of 1.7 (Ref. [10]) and 1.9 KΩ (Ref. [9]) for the AlO and MgO MTJs respectively, considering these values we apply maximum current densities of 1.2×10^7 (AlO) and 1.0×10^7 A/cm^2 (MgO).

In our calculations, we use a time step of 28 fs. Simulations performed with shorter time step gave the same results exactly. The samples where discretized into cells of $2.5\times2.5\times4.0$ nm^3. Simulations have also been performed with cells of $2.0\times2.0\times2.0$ and $2.5\times2.5\times2.0$ nm^3, giving rise to

[a]Also at: Departamento de Fisica Aplicada, Universidad de Salamanca Plaza de la Merced s/n, 37008 Salamanca, Spain; electronic mail: gfinocchio@ingegneria.unime.it

 © 2006 American Institute of Physics
Downloaded 30 Dec 2006 to 88.9.101.30. Redistribution subject to AIP license or copyright, see http://apl.aip.org/apl/copyright.jsp

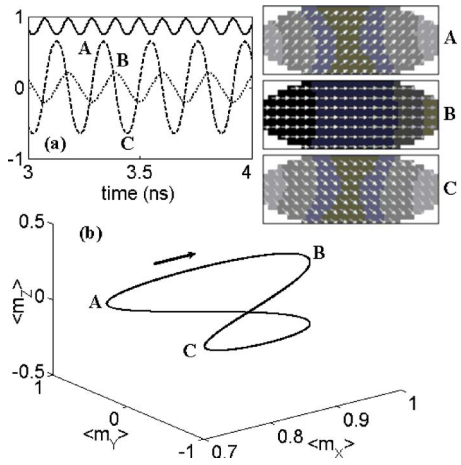

FIG. 1. (Color online) (a) Temporal evolutions of the x (solid line), y (dashed line), and z (dotted line) components of the average magnetization for an applied field $H=50$ mT and a current density $J=-0.97\times10^7$ A/cm^2 (AlO MTJ); (top right) snapshots of magnetization at three different points displayed in (a): A (x minimum, y maximum), B (x maximum, z maximum), and C (x minimum, y minimum); (b) 3D view of the average magnetization motion of the same process.

very similar results, where the magnetization dynamics vary by less than 5%.

An applied field of 50 mT (value close to the average x component of the magnetostatic coupling with the PL), applied along the positive x direction, has been used for the computation of the critical current at zero temperature. These calculations produce $J_{\text{C–AlO}}=1.15\times10^7$ A/cm^2 and $J_{\text{C–MgO}}=0.73\times10^7$ A/cm^2, which are the same for both APS$\rightarrow$PS and *vice versa* processes. The magnetization reversals obtained in both structures occur via nucleation process (not shown), likewise to recently time-resolved imaging at nanoscale of magnetization reversal in spin valves.[11]

Furthermore, for both devices, we observe that currents lower than the critical one are able to drive magnetization dynamics. Figure 1(a) shows the temporal evolution of the x (solid line), y (dashed line), and z (dotted line) components of the average magnetization for an applied field $H=50$ mT and a current density $J=-0.97\times10^7$ A/cm^2 (AlO MTJ). Figure 1 top right) shows snapshots of magnetization configuration at three different points: A (x minimum, y maximum), B (x maximum, z maximum), and C (x minimum, y minimum). As can be noted, this persistent dynamics is given by the oscillation of the spins at the boundaries of the structure. A three-dimensional (3D) view of the average magnetization motion of the same process is displayed in Figure 1(b). A similar results for the MgO MTJ is obtained for a value of current density $J=-0.6\times10^7$ A/cm^2. Figure 2(a) shows the plot of the frequency of microwave oscillations versus the applied field for AlO (solid line, $J=-0.97\times10^7$ A/cm^2) and MgO (dashed line, $J=-0.6\times10^7$ A/cm^2). In both cases, the frequency increases when the field increases (blueshift).[12] These results are in agreement with the experiments related to the microwave oscillations driven by SPC, when the field is applied in plane, in SVs and point-contact geometries.[3,5] Figure 2(b) shows the static loop computed by numerically solving the Brown equation for both MTJs. We obtain a coercivity of 95 mT. We investigated the behavior of the devices at high field regime where the applied fields are larger than the coercivity. We performed simulations at fields of 100, 150, and 200 mT and current

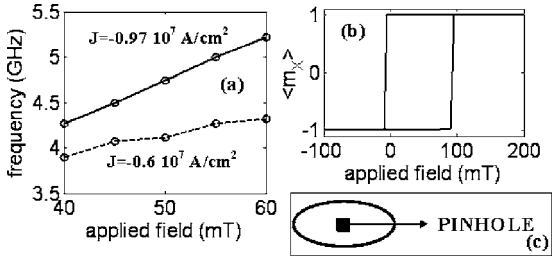

FIG. 2. (a) Plot of the frequency of microwave oscillations vs the applied field for AlO MTJ (solid line, $J=-0.97\times10^7$ A/cm^2) and MgO MTJ (dashed line, $J=-0.6\times10^7$ A/cm^2); (b) static hysteresis loop ($\boldsymbol{H}$,$\langle\boldsymbol{m}_X\rangle$) computed by solving the Brown equation; (c) view of the pinhole location in the elliptical cross section of the MTJ.

density range up to -1.2×10^7 A/cm^2 for AlO MTJ and up to -1×10^7A/ cm^2 for MgO MTJ. In the former MTJ, we observe persistent dynamics regime only at a field of 100 mT and a current density of -1.2×10^7 A/cm^2, it is similar to the one described at low field regime, in all the other cases we have the PS. Concerning the MgO MTJ, all our simulations show that when a current is able to excite microwave oscillations, we obtain a chaotic behavior of the magnetization. For example, Fig. 3(a) shows the y component of the average magnetization due to a SPC $J=-0.3\times10^7$ A/cm^2 and an applied field of 200 mT (MgO MTJ), while Fig. 3(b) shows the relative total power spectrum computed by means of the micromagnetic spectral mapping technique (MSMT).[13,14] As can be noted, the spectrum is very noisy typical of a chaotic signal. We attribute this behavior to the complex domain configurations that we observe during the dynamic process, depending on the time range, there is an alternating of completely different configurations. For example, a vortex which moves in the device together with oscillations of the spins at the boundaries (Fig. 3 top right A), 180° (Fig. 3 top right B) or 360° (Fig. 3 top right C) domain configurations with the wall of the domain propagating through the structure.

Lastly, we performed a study of the influence of a pinhole (placed in the center of the insulator) in the magnetization dynamics [see Fig. 2(c)]. It is modeled as a square cross section (15 nm in side) perpendicular conducting channel through the tunnel barrier. We assumed that the current flows

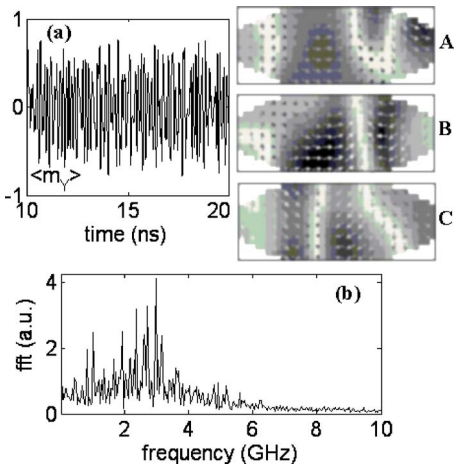

FIG. 3. (Color online) (a) Temporal evolution of the y component of average magnetization for an applied field $H=200$ mT and a current density $J=-0.3\times10^7$ A/cm^2 (MgO MTJ); (b) total spectrum of the above signal computed by means of the MSMT; (top right A–C) snapshots of three different domain configurations of the same dynamic above.

Downloaded 30 Dec 2006 to 88.9.101.30. Redistribution subject to AIP license or copyright, see http://apl.aip.org/apl/copyright.jsp

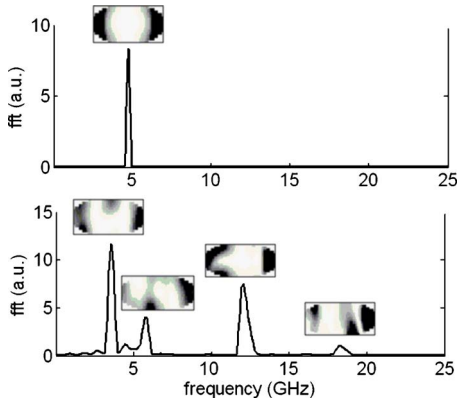

FIG. 4. (Color online) (top) Total spectrum of the magnetization dynamics driven by a SPC $J=-0.97\times10^7$ A/cm^2 and a field of 50 mT (AlO MTJ) together with the 2D spatial distribution of the main mode excited (4.74 GHz); (bottom) total spectrum of the magnetization dynamics driven by a SPC $J=-1.86\times10^7$ A/cm^2 and a field of 50 mT (AlO MTJ), when a squared cross-section pinhole has been introduced in the center of the ellipse, together with the 2D spatial distribution of the main modes excited. The frequencies of the excited modes are 3.56, 5.78, 12, and 18.3 GHz.

through this channel while the rest of the area is to be assumed no conductive.[15] Our main results are (a) the current necessary to excite microwave oscillations is larger than the MTJ with no pinholes and (b) the total spectrum presents more frequency peaks with a complex spatial distribution.

Figure 4 top) shows the total spectrum of the magnetization dynamics driven by a SPC $J=-9.7\times10^7$ A/cm^2 and a field of 50 mT (AlO MTJ), where the frequency peak of the main mode is 4.74 GHz. The small inset shows the two-dimensional (2D) spatial distribution of the power spectral density of that mode (increasing from white to black), it is proportional to spectrum of that cell and that frequency. As can be noted the mode is distributed symmetrically in the ellipse. Figure 4 (bottom) shows the total spectrum (pinhole case) of the magnetization dynamics driven by a SPC $J=-1.86\times10^7$ A/cm^2 and a field of 50 mT (AlO MTJ).[16] The total spectrum presents more peaks and these have a 2D spatial distribution very complex. This difference is mainly attributed to the nucleation process due either to the presence of the pinhole or to the different spatial distributions of the Oersted field.

In summary, we performed a micromagnetic study of the magnetization dynamics driven by SPC and magnetic field in AlO and MgO MTJs. Our results show that for low field regime in both MTJs there are microwave oscillations with a well defined main peak in frequency. The frequency of this peak increases when the applied field increases. In high field regime, similar dynamics to the one of low field regime in AlO MTJs is observed (the current densities are close to the one which gives the breakdown voltage of the barrier). Differently, chaotic behavior of the magnetization is found in MgO MTJs. Lastly, the presence of a pinhole in the MTJs gives rise to two effects: (1) increasing of the minimum current to excite dynamics and (2) existence of several peaks in the frequency spectrum, each of them presenting a complex 2D spatial distribution.

Trends in MTJs magnetization persistent dynamics shown by the full micromagnetic computations exposed in this letter open perspectives for the experimenters in the design of spintronic MTJs nano-oscillators.

The authors are grateful to Gregory Fuchs for helpful discussions. The authors thank Fabio Giroldini for the software support. This work has been partially supported by the Spanish Government under Project No. MAT2005-04287.

[1] J. Slonczewski, J. Magn. Magn. Mater. **159**, L1 (1996); **195**, L261 (1999); **247**, 324 (2002).
[2] L. Berger, Phys. Rev. B **54**, 9353 (1996).
[3] J. A. Katine, F. J. Albert, R. A. Buhrman, E. B. Myers, and D. C. Ralph, Phys. Rev. Lett. **84**, 3149 (2000); J. Grollier, V. Cros, H. Jaffres, A. Hamzic, J. M. George, G. Faini, J. B. Youssef, H. Le Gall, and A. Fert, Phys. Rev. B **67**, 174402 (2003); M. AlHajDarwish, H. Kurt, S. Urazhdin, A. Fert, R. Loloee, W. P. Pratt, Jr., and J. Bass, Phys. Rev. Lett. **93**, 157203 (2004); S. I. Kiselev, J. C. Sankey, I. N. Krivorotov, N. C. Emley, R. J. Schoelkopf, R. A. Buhrman, and D. C. Ralph, Nature (London) **425**, 380 (2003); I. N. Krivorotov, N. C. Emley, J. C. Sankey, S. I. Kiselev, D. C. Ralph, and R. A. Buhrman, Science **307**, 228 (2005); T. Devolder, C. Chappert, P. Crozat, A. Tulapurkar, Y. Suzuki, J. Miltat, and K. Yagami, Appl. Phys. Lett. **86**, 062505 (2005); S. I. Kiselev, J. C. Sankey, I. N. Krivorotov, N. C. Emley, A. G. F. Garcia, R. A. Buhrman, and D. C. Ralph, Phys. Rev. B **72**, 064430 (2005); S. Kaka, Matthew R. Pufall, W. H. Rippard, T. J. Silva, S. E. Russek, J. A. Katine, and M. Carey, J. Magn. Magn. Mater. **286**, 375 (2005).
[4] G. D. Fuchs, N. C. Emley, I. N. Krivorotov, P. M. Braganca, E. M. Ryan, S. I. Kiselev, J. C. Sankey, D. C. Ralph, R. A. Burman, and J. A. Katine, Appl. Phys. Lett. **85**, 1205 (2004); J. S. Moodera and G. Mathon, J. Magn. Magn. Mater. **200**, 248 (1999); Z. Diao, D. Apalkov, M. Pakala, Y. Ding, A. Panchula, and Y. Huai, Appl. Phys. Lett. **87**, 232502 (2005); J. Vogel, W. Kuch, R. Hertel, J. Camarero, K. Fukumoto, F. Romanens, S. Pizzini, M. Bonfim, F. Petroff, A. Fontaine, and J. Kirschner, Phys. Rev. B **72**, 220402(R) (2005); H. Kubota, A. Fukushima, Y. Ootani, S. Yuasa, H. Maehara, K. Tsunekawa, D. D. Djayaprawira, N. Watanabe, and Y. Suzuki, IEEE Trans. Magn. **41**, 2633 (2005); H. Kubota, A. Fukushima, Y. Ootani, S. Yuasa, K. Ando, H. Maehara, K. Tsunekawa, D. D. Djayaprawira, N. Watanabe, and Y. Suzuki, Jpn. J. Appl. Phys., Part 2 **44**, L1237 (2005); R. H. Koch, J. A. Katine, and J. Z. Sun, Phys. Rev. Lett. **92**, 088302 (2004).
[5] W. H. Rippard, M. R. Pufall, S. Kaka, S. E. Russek, and T. J. Silva, Phys. Rev. Lett. **92**, 027201 (2004); O. Ozatay, N. C. Emley, P. M. Braganca, A. G. F. Garcia, G. D. Fuchs, I. N. Krivorotov, R. A. Buhrman, and D. C. Ralph, Appl. Phys. Lett. **88**, 202502 (2006).
[6] L. Torres, L. Lopez-Diaz, E. Martinez, M. Carpentieri, and G. Finocchio, J. Magn. Magn. Mater. **286**, 381 (2005); M. Carpentieri, G. Finocchio, B. Azzerboni, L. Torres, L. Lopez-Diaz, and E. Martinez, J. Appl. Phys. **97**, 10C713, (2005); **99**, 08G522 (2006); G. Finocchio, I. Krivorotov, M. Carpentieri, G. Consolo, B. Azzerboni, L. Torres, E. Martinez, and L. Lopez-Diaz, *ibid.* **99**, 08G507 (2006).
[7] J. Slonczewski, Phys. Rev. B **71**, 024411 (2005).
[8] W. F. Egelhoff, Jr., R. D. McMichael, C. L. Dennis, M. D. Stiles, A. J. Shapiro, B. B. Maranville, and C. J. Powell, Appl. Phys. Lett. **88**, 162508 (2006).
[9] G. D. Fuchs, J. A. Katine, S. I. Kiselev, D. Mauri, K. S. Wooley, D. C. Ralph, and R. A. Buhrman, Phys. Rev. Lett. **96**, 186603 (2006).
[10] G. D. Fuchs, I. N. Krivorotov, P. M. Braganca, N. C. Emley, A. G. F. Garcia, D. C. Ralph, and R. A. Buhrman, Appl. Phys. Lett. **86**, 152509 (2005).
[11] Y. Acremann, J. P. Strachan, V. Chembrolu, S. D. Andrews, T. Tyliszczak, J. A. Katine, M. J. Carey, B. M. Clemens, H. C. Siegmann, and J. Stöhr, Phys. Rev. Lett. **96**, 217202 (2006).
[12] A. N. Slavin and P. Kabos, IEEE Trans. Magn. **41**, 1264 (2005).
[13] It consists on performing a fast Fourier transform of the temporal evolution of magnetization for each computational cell $S_Y(x_l,y_m,z_n,f)=\Sigma_h m_Y(x_l,y_m,z_n,t_h)e^{-j2\pi ft_h}$, then the total spectrum is computed by the following: $S_T(f)=1/N\Sigma_{l,m,n}|S_Y(x_l,y_m,z_n,f)|^2$ (y component of magnetization); the indices l, m, and n identify a computational cell, t_h is the discretized time step, f is the frequency, and N is the total number of the cells.
[14] M. Grimsditch, L. Giovannini, F. Montoncello, F. Nizzoli, G. Leaf, H. Kaper, and D. Karpeev, Physica B **354**, 266 (2004); R. D. McMichael, M. D. Stiles, J. Appl. Phys. **97**, 10J901 (2005); D. V. Berkov and N. L. Gorn, Phys. Rev. B **72**, 094401 (2005); **71**, 052403 (2005).
[15] J. G. Zhu, J. Appl. Phys. **97**, 10N703 (2005).
[16] This current is the smaller which gives persistent magnetization dynamic at that field when a pinhole has been introduced in the device.

Downloaded 30 Dec 2006 to 88.9.101.30. Redistribution subject to AIP license or copyright, see http://apl.aip.org/apl/copyright.jsp